Molecular features of cephalosporins important for activity against antimicrobial-resistant *Neisseria gonorrhoeae*

Jonathan M. Turner[1], **Kristie L. Connolly**[2], **Kate E. Aberman**[3,^], **Joseph C. Fonseca II**[3,#], **Avinash Singh**[1], **Ann E. Jerse**[2], **Robert A. Nicholas**[3,4], **Christopher Davies**[1,*]

[1]Department of Biochemistry and Molecular Biology, Medical University of South Carolina, Charleston, South Carolina 29425

[2]Department of Microbiology and Immunology, Uniformed Services University, Bethesda, MD 20814

[3]Department of Pharmacology, University of North Carolina at Chapel Hill, Chapel Hill, NC 27599

[4]Department of Microbiology and Immunology, University of North Carolina at Chapel Hill, Chapel Hill, NC 27599

Abstract

The increasing prevalence of *Neisseria gonorrhoeae* strains exhibiting decreased susceptibility to extended-spectrum cephalosporins (ESCs) presents a challenge for the successful treatment of gonorrhea infections. To address this challenge, we evaluated a panel of 23 cephalosporins against penicillin-binding protein 2 (PBP2) from the ESC-resistant (ESC^R) *N. gonorrhoeae* strain H041 to determine which molecular features are important for antimicrobial activity. Structure-activity relationships (SAR) developed from acylation rate constants against PBP2 and antimicrobial susceptibilities against the ESC^R H041 strain of *N. gonorrhoeae,* and interpreted against docking models, reveal that cephalosporins possessing large, lipophilic R_1 side chains and electronegative R_2 side chains with planar groups are associated with higher acylation rates against PBP2, but also that these same amphipathic features can lower antimicrobial activity. Based on these studies, we tested cefoperazone, one of the most effective ESCs for targeting PBP2, in the female mouse model infected with H041, and showed that it was equally or more effective than ceftriaxone or gentamicin for clearing infections. Taken together, our results reveal that two FDA-approved agents (cefoperazone, ceftaroline) and one FDA qualified infectious disease product (ceftobiprole)

[*]Corresponding author: Department of Biochemistry & Molecular Biology, University of South Alabama, 5795 USA Drive North, Mobile, AL 36688. Tel +1 (651) 460-6659; cdavies@southalabama.edu.
[^]Present address: National Institute of Allergy and Infectious Diseases, Immunobiology Section, 33 North Drive, Bethesda MD 20814
[#]Present address: Morehouse College, 830 Westview Drive SW, Atlanta, GA 30314

have potential as first-line treatments for gonorrhea and provide a framework for the future design of cephalosporins with improved activity against ESC-resistant *N. gonorrhoeae*.

Keywords

Neisseria gonorrhoeae ; penicillin-binding protein 2; cephalosporins; structure-activity relationship; molecular docking

Gonorrhea is one of the most common sexually transmitted infections (STIs), with over 800,000 cases reported annually in the U.S. and 78 million cases reported worldwide [1–2]. Untreated gonococcal infections result in serious sequelae, including pelvic inflammatory disease in women, epididymitis in men, and gonococcal arthritis and increased risk of contracting and transmitting HIV in both sexes [3–4]. Due to the emergence of antimicrobial resistance, penicillin, tetracycline and fluoroquinolone antibiotics were withdrawn as recommended therapies for gonococcal infections, leaving the extended-spectrum cephalosporins (ESCs) cefixime or ceftriaxone as the mainstay of treatment for several years. Their efficacy, however, is being threatened by the emergence of *N. gonorrhoeae* strains exhibiting decreased susceptibility to ESCs, beginning with strains of reduced susceptibility [5–8] and followed by clinically resistant strains (ESC[R]) [9–11]. There have since been numerous reports of verified treatment failures with ESCs across the world [12–15]. As a result, many public health agencies withdrew cefixime as a first-line treatment for gonorrhea, and now recommend ceftriaxone in combination with azithromycin [16–19]. Even so, there are already reports of treatment failures with this dual regimen [20–21].

The pharmacologic receptors for cephalosporins are the penicillin-binding proteins (PBPs), a group of transpeptidases that catalyze the cross-linking of the peptide moieties in peptidoglycan [22–23]. Peptidoglycan is an essential component of the bacterial cell wall and plays a major role in cell shape, growth, and division [24]. PBPs are generally classified as high-molecular-mass (HMM) and low-molecular-mass (LMM), with the HMM PBPs being essential, and the LMM being non-essential. HMM PBPs can be further divided into Class A PBPs, which are bifunctional glycosyl transferases/transpeptidases, and Class B PBPs, which only catalyze transpeptidase activity. LMM PBPs are generally Class C endopeptidases or carboxypeptidases. Four PBPs are encoded by the genome of *N. gonorrhoeae*: PBP1 (Class A) and PBP2 (Class B) are both essential, whereas PBP3 and PBP4 (Class C) are nonessential [25–26]. Since PBP2 is inhibited at tenfold lower penicillin concentrations than PBP1, it is the primary target for penicillin in susceptible strains [25].

The active site of PBPs contains three conserved motifs: SxxK, SxN, and KTG (where x denotes a variable residue) [27]. The reaction catalyzed by PBPs involves three steps: 1) Michaelis-Menten non-covalent binding of peptide substrate, 2) formation of an acyl-enzyme complex, and 3) attack of the complex by another peptide or water to yield a peptide cross-link or a shortened substrate unable to undergo further cross-linking (deacylation). Since the reaction is covalent, affinity cannot be measured separately from acylation and the kinetics are therefore measured by the second order rate of acylation, k_2/K_S [28–29]. In *N. gonorrhoeae*, the peptide substrate is L-Ala-D-isoGlu-m-DAP-D-Ala-D-Ala, where m-DAP is meso-diaminopimelic acid. The nucleophilic serine hydroxyl group of the SxxK motif

attacks the carbonyl carbon of the penultimate D-Ala residue of the peptide substrate to form the acyl-enzyme complex. As substrate mimics, β-lactams react in a similar way as peptide substrate, with the serine nucleophile attacking the carbonyl carbon of the β-lactam ring. The difference between the two reactions is that deacylation is blocked after acylation by β-lactams and the PBP is rendered inactive due to prolonged occupation of the active site.

For most *N. gonorrhoeae* strains, β-lactam resistance is acquired via mutations in several chromosomally encoded genes. These include mutations in the porin PorB$_{1B}$ [30], the *mtr* locus that increases expression of the MtrCDE efflux pump [31], *ponA*, which encodes PBP1 [32], and in *penA*, which encodes PBP2 [33]. Of these, the major determinant for cephalosporin resistance is acquisition of so-called mosaic *penA* alleles. These arise from recombination events with *penA* genes from multiple commensal *Neisseria* species and result in approximately 60 amino acid changes compared to wild-type PBP2 from the susceptible strain FA19 [8, 34–35]. The first reported ESC^R strain, called H041, was isolated in Japan [9]. In common with most *N. gonorrhoeae* strains, the cephalosporin resistance of H041 results from chromosomally mediated mechanisms and not expression of a β-lactamase [35]. Ceftriaxone exhibits an MIC of 2 μg/mL for H041, an increase of 3,000-fold compared to strain FA19, and well above the EUCAST breakpoint of 0.125 μg/ml [35]. When the wild-type *penA* gene in FA19 is replaced with the mosaic *penA* gene from H041 (*penA41*) by allelic exchange, the minimum inhibitory concentration (MIC) of ceftriaxone increases by 570-fold and is beyond the breakpoint for this antibiotic [36]. Strikingly, this increase occurs in the absence of other resistance determinants, establishing PBP2 as the main cause of treatment failures with ESCs. The crystal structure of PBP2 from H041 has been solved and reveals that mutations responsible for resistance both lower affinity for cephalosporins and create an energetic barrier against acylation by ESCs by restricting conformational changes [37].

The cephalosporins are a structurally diverse class of antibiotics that are grouped for convenience into approximate generations based on their timeline of development, and presence of chemical modifications that affect activity and antimicrobial spectrum (Figure 1). While the third-generation agents cefixime and ceftriaxone have been the most commonly prescribed cephalosporins for gonorrhea over recent years, few other cephalosporins have been tested against ESC^R strains. This is especially true for fourth- (*e.g.*, cefepime) and fifth-generation (*e.g.,* ceftaroline and ceftobiprole) agents that have been approved relatively recently. Building structure-activity relationships (SAR) for cephalosporins against their PBP2 target from an ESC^R strain of *N. gonorrhoeae* offers the potential to address ESC-resistant *N. gonorrhoeae* in two ways: it may reveal existing FDA-approved cephalosporins that exhibit efficacy against ESC^R strains and suggest how the efficacy of specific cephalosporins can be improved by chemical modification.

Here, we report a quantitative structure-activity relationship (QSAR) of 22 cephalosporins for inhibition of PBP2 from H041 and antimicrobial activity against *N. gonorrhoeae*. The data reveal key features of cephalosporins that enhance formation of the pre-covalent PBP2-β-lactam complex, as well as those that may independently hinder or enhance antimicrobial activity. The study also reveals that FDA-approved agents cefoperazone (Cefobid, Pfizer) and ceftaroline (Teflaro, Allergan), as well as FDA qualified infectious disease product (QIDP) ceftobiprole (Zevtera, Basilea), acylate mosaic PBP2 at higher rates

than ceftriaxone, and that cefoperazone exhibits higher antimicrobial activity against H041. Overall, our data reveal there is considerable potential in adopting and/or adapting these cephalosporins as anti-gonococcal agents to address ESC-resistant *N. gonorrhoeae*.

Results

Docking of cephalosporins to tPBP2[H041] reveals conserved ligand-target interactions.

To identify residues of PBP2 involved in the recognition of cephalosporins in the precovalent complex, cephalosporins were computationally docked to the active site of tPBP2[H041]. A pharmacophore constraint was used to confine the β-lactam ring system to the area around the Ser310 nucleophile and the oxyanion hole formed by the amide nitrogens of Ser310 and Thr500, and the refined poses for all compounds remained largely within the volume specified (Figure S1). Protein-ligand interaction fingerprints (PLIF) of all poses were generated for each molecule, and their interactions with individual residues were analyzed by frequency (Figure 2A) and type of interaction (Figure 2B), and the predominant interactions were used to generate a consensus pharmacophore (Figure 2C). For all cephalosporins, S310 and T500 contact the β-lactam carbonyl oxygen with side chain and main chain hydrogen-bonding interactions, respectively, while K313 and K497 are predominantly involved in side chain ionic interactions with the cephem C4 carboxylate group. In addition, most of the cephalosporins contact T347, K361, S483, and S545. The C4 carboxylate moiety participates in additional hydrogen bonding interactions with the hydroxyl group of S483, and in most poses, the sulfur of the cephem dihydrothiazine ring participates in weak hydrogen bonding with the side chain hydroxyl group of T347. Electronegative elements of many of the cephalosporin R_2 groups (at C3) make side chain and main chain polar contacts with K361, including the thiotriazinone (TTZ) moiety of ceftriaxone (Figure 3A). Finally, the common amide moiety of all R_1 groups (at C7) makes variable polar contacts within the active site. In some poses, the amide nitrogen participates in hydrogen bonding with S545 and the carbonyl oxygen with N364, while in others, the C7-N bond is rotated such that the carbonyl oxygen interacts with S545. This rotation also affects the position of the R_1 aromatic ring systems of several cephalosporins, leading to two positions of the aminothiazole group: one in which it reaches toward the hydrophobic pocket formed by Y422 on the α8-β2f loop, and one in which it projects toward Y544 on the β5-α11 loop (Figure 3B).

Closer inspection of the poses revealed two possible binding modes for all cephalosporins examined: a "major pose" was observed for approximately 60% of poses (131/220), and a "minor pose" for 40% (89/220) (Figure 4). While there appear to be to no differences in docked energy scores for the major pose (-6.39 ± 0.56 kcal·mol^{-1}) over the minor pose (-6.54 ± 0.79 kcal·mol^{-1}, $p = 0.17$), compounds with faster acylation rates tended to occupy the minor pose (OR = 0.38, $p = 0.01$). Representative examples of each pose for ceftriaxone and cefoperazone are shown in Figure 5. In the major pose, the C4 carboxylate of the cephalosporin interacts with Oγ of S483 and K497, and the β-lactam ring is positioned away from the serine nucleophile (Figure 5A and C). Connolly surface renderings show that, in this position, the C4 carboxylate fits into a small pocket bordered by the side chains of S362, S483, and K497 (Figure S2). In the minor pose, the carboxylate is situated within the

hydrogen bonding network created by K313, and S310, and the β-lactam ring is relatively closer to S310 (Figure 5B and D). Interestingly, neither pose overlaps with the binding of ceftriaxone observed in the crystal structure of tPBP2^{H041} acylated by this antibiotic [37] (Figure S3). Of the two binding modes, the minor pose appears more favorable for initiation of the acylation reaction than the major pose because the Oγ of S310 is relatively closer to the β-lactam carbonyl.

Cephalosporins exhibit a range of acylation rates against tPBP2^{H041}.

The inactivation of PBPs by β-lactams results in the formation of a long-lived covalent bond between the serine nucleophile and antibiotic. This means that the equilibrium binding affinity (K_s) cannot be measured separately from the rate of acylation (k_2), and reactions are therefore monitored by the second-order rate of acylation, k_2/K_s. While it is conceivable that the measured k_2/K_s values could be influenced by a high off rate (k_3), in practice, the rates of deacylation for PBPs are typically very low and considered insignificant for the overall reaction [28–29, 38]. In support of this, the measured k_3 rates for the acylated ceftriaxone complexes of wild-type PBP2 (tPBP2^{WT}) and tPBP2^{H041} are 2.8×10^{-6} sec^{-1} and 8.1×10^{-5} sec^{-1}, respectively [37], and not on a timescale where a steady-state equilibrium is established when compared to k_2/K_s values for cephalosporins, which are typically in the range of 10^2-10^4 M^{-1} s^{-1} for tPBP2^{H041} (see below).

As a prerequisite to determining k_2/K_s for the panel of cephalosporins against tPBP2^{H041}, we measured k_2/K_s for Bocillin-FL against tPBP2^{H041} using a time-dependent gel-based assay (Figure S4). The obtained value, 275 ± 9 M^{-1}s^{-1}, is consistent with values previously reported for [^{14}C]penicillin G against PBP2 from H041 [36]. k_2/K_s was then determined for each cephalosporin with a gel-based competition assay using Bocillin-FL. The 23 cephalosporins exhibited a wide range of activities against tPBP2^{H041} (Table 1), with acylation rates ranging from 0 to over 10,000 M^{-1}s^{-1}. Three of the cephalosporins exhibited 2-7 fold faster rates of acylation than ceftriaxone ($1,710 \pm 320$ M^{-1s-1}). These were cefoperazone ($11,800 \pm 1,300$ M^{-1}s^{-1}), ceftaroline ($10,900 \pm 1,700$ M^{-1}s^{-1}), and ceftobiprole ($3,230 \pm 190$ M^{-1}s^{-1}). Ceftizoxime exhibited activity comparable to that of ceftriaxone ($1,000 \pm 210$ M^{-1}s^{-1}), whereas several other cephalosporins exhibited slightly slower rates of acylation, including cefotaxime (880 ± 120 M^{-1}s^{-1}), ceftazidime (780 ± 150 M^{-1}s^{-1}), cefixime (720 ± 60 M^{-1}s^{-1}), and cefpodoxime (590 ± 90 M^{-1}s^{-1}). The remaining cephalosporins exhibited very slow acylation rates; in fact, for four of these, cephalexin, cefazolin, cephalothin, and cephaloridine, rates could not be measured.

Examining the acylation data qualitatively, it appears that the R$_1$ side chain has a significant impact on tPBP2^{H041} acylation rate, as seen in pairwise comparisons of compounds with identical R$_2$ side chains (Table S1). These pairings exhibit up to 3,000-fold differences in activity (*e.g.,* cefoperazone versus cefmetazole). By contrast, the R$_2$ side chain has a much lower impact, as evidenced by the narrow range of values obtained for cephalosporins containing diverse R$_2$ side chains in the presence of the same 2-(2-aminothiaozol-4yl)-2-(alkoxyimino)acetyl (ATAO) R$_1$, *e.g.* ceftriaxone and cefotaxime.

Antimicrobial activity of tested cephalosporins against N. gonorrhoeae H041.

Minimum inhibitory concentrations (MICs) against *N. gonorrhoeae* H041 were determined for the panel of cephalosporins by the agar dilution method (Table 1). The tested compounds exhibited varying degrees of antimicrobial potency, ranging from 1 to >32 μg/mL. Consistent with the acylation data, cefoperazone showed slightly more inhibition of bacterial growth than ceftriaxone (1 vs 2 μg/mL), albeit within the error of dilution. Despite their rapid target acylation rates against tPBP2[H041], the MICs for ceftaroline and ceftobiprole were similar or only slightly higher compared to ceftriaxone. By contrast, cefdinir and cefoxitin, which both exhibit relatively low acylation rates against tPBP2[H041], inhibited the growth of H041 at concentrations comparable to ceftriaxone (MIC = 2 and 4 μg/mL, respectively). The anti-gonococcal activity of the remaining cephalosporins was generally weaker, falling in the range of 8 to 16 μg/mL. Cephalothin, ceftazidime, cefaclor, cefsulodin and cephalexin were exceptionally poor antimicrobials, and could not inhibit growth of H041 except at concentrations of 32 μg/mL or more. In general, antimicrobial potency of the cephalosporins correlated relatively poorly with acylation rate, most likely because MICs are also determined by i) the degree of permeation through porins, ii) their capacity as substrates for the MtrCDE efflux pump, and iii) whether they target PBP1, the other essential PBP in *N. gonorrhoeae*.

Quantitative structure-activity relationship (QSAR) for second-order acylation rate constant.

Correlation of acylation data for the 18 cephalosporins with measurable acylation rates with their 2D molecular descriptors yielded a partial least squares (PLS) model with an r^2 of 0.995 and a cross-validated r^2 of 0.957 (Figure S5). 3D descriptors from the docked poses were not included in these calculations because two binding modes had emerged from the docking. In addition to its high degree of predictability within the training set, the PLS model successfully predicts minimal activity for five cephalosporins absent from the training set that have unmeasurable acylation rates against tPBP2[H041] (Table S2). To assess the probability of chance correlation, *y*-randomization was performed, in which activity values are randomly assigned to a structure. This yielded an r^2 of 0.849 and a cross-validated r^2 of 0.064 (Figure S5), showing that correlations seen in the model are not random.

The PLS model shows that the *vdw_area* and *Kier1* descriptors are the dominant contributors, indicating that van der Waals surface area and shape of the R_1 substituent are important drivers of second-order acylation rates of tPBP2[H041] by cephalosporins, with large, modestly unsaturated groups being favored (Table 2). Other features of the R_1 substituent, including overall shape (*zagreb*), connectivity (*chi0v*), and topology (*KierA2*), were also found to correlate with high activity. Overall, the data indicate that active molecules possess an R1 group with a high degree of unsaturation and cyclicity, with modest heteroatom counts and branching. Interestingly, we observe a high degree of collinearity between the descriptors contributing the most to activity (Figure S6), consistent with these features being important for activity.

Given the dominance of the *vdw_area* and *Kier1* in the QSAR, we constructed a second model using only these two descriptors (Figure S7). While a positive correlation between

experimental and predicted activity was observed, the minimal model tends to overpredict the acylation rates of slower cephalosporins. For instance, the model predicts the k_2/Ks of cefsulodin to be 51 M^{-1} s^{-1}, whereas its measured value is 0.8 ± 0.1 $M^{-1}s^{-1}$. This suggests that although the additional descriptors contribute relatively less to activity, they do increase the overall accuracy of the PLS model.

In contrast to R_1, the PLS model shows that the R_2 side chain makes relatively less contribution to acylation, but does have some effect (Table 2). Contributions by the *SlogP_VSA7*, *a_acc* and *G_CUT_PEOE_2* descriptors show that the hydrophobicity of R_2 groups is important, as well as the presence of hydrogen bond acceptors and partial positive charge. The latter may be an indirect result of inductive effects by electronegative atoms in R_2 of highly active compounds.

As a validation of the PLS model, we examined its predictive value for cefpiramide, which was not included in the set of 22 cephalosporins. The structure of this cephalosporin is highly similar to that of cefoperazone, with the only difference being a methylhydroxypyridine ring in place of dioxopiperazine, and thus might be expected to exhibit a similar acylation rate against tPBP2[H041]. Contrary to this expectation, the PLS model predicted low activity for cefpiramide (3.2 $M^{-1}s^{-1}$) and this was borne out experimentally because the k_2/Ks was found to be 100-fold lower than cefoperazone (120 $\pm$ 14 *vs* 11,800 $\pm$ 1,300 $M^{-1}s^{-1}$). Hence, while the observed value deviates somewhat from the predicted value, the model accurately predicts cefpiramide to be of low activity, suggesting that it is capable of parsing out subtle features that modulate acylation.

Quantitative-structure activity relationship (QSAR) for antimicrobial activity against Neisseria gonorrhoeae H041.

Correlation of MIC data for the 21 cephalosporins with their 2D molecular descriptors yielded a partial least squares (PLS) model with an r^2 of 0.999 and a cross-validated r^2 of 0.951 (Figure S5). As with the second-order rates of acylation, *y*-randomization was performed in order to determine the probability of chance correlation, yielding an r^2 of 0.919 and a cross-validated r^2 of 0.002 (Figure S5). Some of the features important for acylation also contribute to antimicrobial activity, including shape and topology (*i.e. KierFlex*, *zagreb*, *chi1v_c*). On the other hand, whereas lipophilicity of R_1 is a driver for acylation rate, antimicrobial activity is enhanced most by the overall hydrophilicity of the molecule, including more hydrogen-bonding elements (*a_donacc*), increased water solubility (*h_logS*), and more negative formal charge (*FCharge*) (Table 3). This trend in favor of hydrophilicity can be seen in several surface area descriptors as well, which show that significant contribution by hydrophobic atoms is unfavored (*Q_VSA_HYD*, *SlogP_VSA4*).

Lys361 is important for recognition of the R_2 side chain of cephalosporins.

As noted above, the docking data reveal a potential interaction between K361, located on the α4 helix in PBP2 and the residue immediately preceding the SxN motif, and polar R_2 side chains (Figure 3A). To examine this position more closely, we aligned a series of class B PBPs from a broad range of Gram-negative bacteria. As seen in Figure S8, a positively

charged residue is highly conserved at this position, suggesting that it may be important for transpeptidase activity of Class B PBPs.

To determine its influence on binding to tPBP2^{H041}, Lys361 was mutated to Glu, and the acylation rates of several cephalosporins with representative electronegative or electropositive R_2 side chains were determined. The second-order acylation rate of Bocillin-FL against tPBP2^{H041}-K361E was 57 ± 1 $M^{-1}s^{-1}$, a 5-fold decrease compared to the native enzyme (Figure S4). The second-order acylation rates of ceftriaxone (290 ± 70 $M^{-1}s^{-1}$) and cefoperazone (370 ± 60 $M^{-1}s^{-1}$) were both markedly lower against the K361E mutant, with reductions of 6-fold and 32-fold, respectively (Table 4). Ceftazidime (560 ± 180 $M^{-1}s^{-1}$) and cefepime (410 ± 130 $M^{-1}s^{-1}$) also exhibited lower acylation rates, although less pronounced. When this mutation is modeled *in silico* and the above docking protocol repeated, the generated poses for ceftazidime and cefepime position R_2 toward the mutated residue due to electrostatic attraction, whereas the R_2 side chains of ceftriaxone and cefoperazone become oriented away from this region (Figure S9). These data indicate a binding mode in the pre-covalent state in which the R_2 side chain of cephalosporins binds the shallow cleft between the β2c-β2d loop and the α10-β3 loop (Figure 3A).

Cefoperazone treatment is efficacious in a murine model of gonococcal infection.

As noted above, cefoperazone exhibited an acylation rate against tPBP2^{H041} higher than ceftriaxone, suggesting it may have therapeutic potential to treat gonorrhea. To examine this question, we used previously modeled PK data for ceftriaxone [39] to predict an effective dosing regimen for cefoperazone using a well-characterized murine infection model [40]. Lower genital tract infection was established with *N. gonorrhoeae* strain H041 in female BALB/c mice for two days and then 120, 60, or 20 mg/kg of cefoperazone was given three-times daily (TID) for one day at 8-hour intervals by the intraperitoneal route. Results were compared to mice given ceftriaxone (60 mg/kg, TID; comparator control), endotoxin-free water (TID, vehicle control) or gentamicin (48 mg/kg, once a day for 5 consecutive days (5QD); positive control). The 120 mg/kg TID cefoperazone dosing regimen resulted in 100% culture negativity by day 3 post-treatment, with a mean time-to-clearance of 2.1 days ($n = 9$) (Figure 6). This level of efficacy was similar to that previously reported for ceftriaxone administered using an identical regimen against this strain [39]. It was significantly more effective than the vehicle control (n = 10, log-rank $p < 0.0001$ versus cefoperazone) and also gentamicin, which resulted in 100% culture negativity by day 4 after initiation of treatment, with a mean time-to-clearance of 3.1 days (n = 8, log-rank $p = 0.02$ versus cefoperazone). A trend for a dose response was observed (Log Rank test for trend) and the 60 mg/kg and 20 mg/kg TID regimens were significantly more effective than the vehicle control (n = 10 for each group, log rank $p = 0.003$ and 0.01 versus cefoperazone), although not more than gentamicin and did not lead to 100% clearance of H041 infection during the 8 day study period. Quantitative differences in colonization load were seen beginning on day 1 for cefoperazone-treated groups compared to vehicle control (two-way RM ANOVA $p < 0.01$) and on day 2 for the gentamicin-treated group (two-way RM ANOVA $p < 0.01$).

Discussion

The goal of the current work was to elucidate which features of the cephalosporin class of β-lactam antibiotics are important for antimicrobial activity against cephalosporin-resistant *Neisseria gonorrhoeae* H041 via inhibition of PBP2. We observed that the structure of the R_1 C7 acylamino side chain of cephalosporins has a profound effect on the second-order rate of tPBP2[H041] acylation, while the R_2 C3 side chain plays a subtler role. Molecular docking simulations of the pre-covalent ligand-receptor complex showed that aromatic and hydrophobic groups on R_1 extend toward a hydrophobic patch of the tPBP2[H041] active site, and electronegative elements of R_2 interact with K361. We also observed that antimicrobial activity correlates minimally with tPBP2[H041] inhibition but is complicated by the additional resistance mechanisms present in the organism. Finally, we demonstrated that cefoperazone acylates tPBP2[H041] at a rate 7-fold faster than ceftriaxone and exhibited comparable activity to ceftriaxone against *N. gonorrhoeae* H041 both *in vitro* and *in vivo*.

Contributions of R_1 to tPBP2[H041]-cephalosporin complex formation.

In this study, we reveal a key role for R_1 structure and properties in the second-order rate of acylation of tPBP2[H041]. In the first instance, the unfavorable contributions of several atomic lipophilicity descriptors indicate that highly hydrophobic moieties are not well tolerated. At the same time, however, the atomic molar refractivity descriptors show that this region also cannot be extremely polar. It therefore appears that the R_1 side chain should contain groups of modest hydrophobicity, such as aromatic- and heteroaromatic ring-containing systems, with additional advantage conferred by hydrogen bonding (*e.g.*, interaction of the acylamino moiety with the amide sidechain of N364 as mimicry of the peptide substrate). In addition, the total van der Waals surface area of the R_1 group contributes positively, suggesting a critical role for size of the cephalosporin. In support of this, the larger (van der Waals volume, V>400 Å^3) and more lipophilic (distribution coefficient, $logD_{7.4}$ = 0.6) 2,3-dioxopiperazinyl R_1 of cefoperazone exhibits a dramatically higher acylation rate than cephalosporins containing ATAO side chains (van der Waals volume V ~ 200 Å^3, distribution coefficient $logD_{7.4}$ = −0.7) present in many third-generation cephalosporins, as well as the chemically similar thiadiazolyl variants possessed by fifth-generation agents.

Shape and topology also play critical roles, with high degrees of unsaturation and cyclicity being associated with higher rates of acylation. Illustrating this trend is the vast difference in acylation rates between cefmetazole, which has a negligible acylation rate and is the only cephalosporin in our study lacking a ring system on R_1, and cefoperazone, which has two ring systems and exhibits the highest rate among the cephalosporins tested. There is also a preference for modest numbers of heteroatoms in the R_1 group, as well as a moderate degree of branching. The former is illustrated by the low activity conferred by the tetrazolyl R_1 of cefazolin, and the latter is apparent from differences in acylation rates between compounds with 2-unsubstituted acylamino groups (*e.g.*, cephalothin and cephaloridine) and those with a single branch point at this position (*e.g.*, ceftriaxone and cefoperazone). It is possible that the preference for cephalosporins with a branched R_1 side chains reflects the forking of the natural peptide substrate at a similar position. Energy score analysis of docking data for R_2-paired compounds suggests that the R_1 side chain impacts pre-covalent Michaelis

complex formation by affecting affinity for tPBP2^{H041} rather than acylation (Figure S10). With the exception of ceftizoxime and ceftibuten, the faster acylating compound of each pair shows a more favorable binding energy with the tPBP2^{H041} active site.

The observation that size and shape are dominant predictors of effective tPBP2^{H041} acylation suggests that specific interactions with variable regions of R_1 may be less critical for complex formation and that, perhaps, there are additional unidentified features not present in our dataset that enhance acylation rate. In this study, we limited ourselves to FDA-approved cephalosporins and QIDP ceftobiprole, but testing of additional and more diverse cephalosporins may yield more information. We could not test the upper bounds of size, as there are no commercial cephalosporins with R_1 larger than cefoperazone, and the same is true for alternate branching patterns, as cephalosporins in use either have a single branch point or lack one altogether.

Previous studies have also indicated that the R_1 side chain is an important driver of affinity against PBPs. In a qualitative structure-activity relationship of penicillin analogues against *E. faecium* PBP5, it was found that azlocillin (k_2/K_s = 15 M^{-1}s^{-1}) exhibited a higher rate than piperacillin (k_2/K_s = 2.2 M^{-1}s^{-1}), ampicillin (k_2/K_s = 1.8 M^{-1}s^{-1}), or Bocillin-FL (k_2/K_s = 1.1 M^{-1}s^{-1}) [41]. Similarly, in a separate study of *Streptomyces* R61, penicillin G (k_2/K_s = 10,300 M^{-1}s^{-1}) was shown to be more potent than penicillin V (k_2/K_s = 1,500 M^{-1}s^{-1}), carbenicillin (k_2/K_s = 830 M^{-1}s^{-1}), and ampicillin (k_2/K_s = 107 M^{-1}s^{-1}) [28]. Since the β-lactams examined in these experiments were all penicillin analogues, which possess geminal dimethyl groups at the R_2 position, one can conclude that differences in activity are imparted by R_1.

The strong influence of the R_1 group on the activities of cephalosporins is important to consider in light of recent new understanding of how PBP2 is acylated by ESCs. Structures of tPBP2^{WT} acylated by cefixime or ceftriaxone reveal significant movement of the β3-β4 loop toward the active site, where several residues form a cluster around the aminothiazole ring, and such interactions may contribute to the affinity of ESCs for PBP2 [42]. The situation is very different in tPBP2^{H041} because movement of the loop appears restricted by mutations conferring resistance to ESCs, resulting in fewer interactions involving the aminothiazole in the acylated complex [37]. Our docking data for tPBP2^{H041} suggest that hydrophobic and aromatic components of R_1 extend toward a hydrophobic patch formed by the side chains of F420 and Y422, with minimal involvement of residues from the β3-β4 loop. Overall, this suggests that the most effective cephalosporin for acylation of tPBP2^{H041} is one whose R_1 can induce movement of the β3-β4 loop to form more extensive contacts with the active site.

Given that the analysis includes only FDA-approved cephalosporins and QIDP ceftobiprole, which have been extensively optimized by medicinal chemistry, it is reasonable to consider whether the correlations seen are simply the result of this process. For example, cephalosporins of more advanced generations possess a single branch point. However, most cephalosporins preceding the fifth generation were optimized for antimicrobial activity rather than target inhibition, and many (*i.e.,* third- and fourth-generation agents) were specifically modified to improve their Gram-negative spectrum of activity, a measure that tends to correlate poorly with target inhibition due to a need for periplasmic accumulation

[43–46]. Moreover, there are third- and fifth-generation agents optimized in this way that exhibit very poor acylation of tPBP2^{H041} (*e.g.*, ceftolozane, ceftibuten, and cefdinir).

Contributions of R_2 to tPBP2^{H041}-cephalosporin complex formation.

We also found that structural variations in the R_2 groups of cephalosporins can affect the rates of acylation, albeit to a lesser extent than R_1. First, R_2 groups with planar or cyclic moieties correlate with higher k_2/K_s values. In fact, the R_2 groups of the compounds with the highest k_2/K_s values (*i.e.,* cefoperazone, ceftaroline, ceftobiprole, and ceftriaxone) all contain planar moieties with extended ring systems, conferring several-fold increases in acylation when compared with compounds of similar R_1 group that lack R_2 rings (*e.g.*, ceftobiprole versus cefdinir). Second, the hydrogen bonding capacity of R_2 also appears to affect acylation, as exemplified by the thiotriazinone (TTZ) moiety, which forms a hydrogen bond with K361, conferring a 1.5- to 3-fold increase in k_2/K_s over other ATAO-containing cephalosporins, likely by decreasing K_s. Our docking data suggest that electronegativity and the hydrogen-bonding capability of R_2 enhances the binding affinity for tPBP2^{H041}. The R_2 group can also contribute via electron-withdrawing inductive effects through the conjugated cephem system [47–48], thereby activating the β-lactam carbonyl for more rapid acylation. This is best illustrated by the differences in acylation rate between cefaclor (29 ± 4 M^{-1}s^{-1}) and cephalexin (~0.3 M^{-1}s^{-1}), which have identical R_1 groups but possess R_2 groups with opposite inductive effects.

Finally, we found no correlation between the presence or absence of a leaving group at the C3 position and k_2/K_s. C3 substituents are expelled by resonance after ring-opening, and cephalosporins containing these are thought to form more stable acyl-enzyme complexes, thereby decreasing the rate of deacylation (k_3) and subsequent regeneration of the PBP in its *apo* form [49–50]. The absence of any correlation is consistent with the C3 leaving group affecting k_3 but not the rate of acylation. Nevertheless, the leaving group should still be taken into consideration when selecting or designing antigonococcal therapeutics in order to prevent agents being compromised by a high k_3. This is potentially relevant for PBP2 given that tPBP2^{H041} has an enhanced rate of deacylation compared to tPBP2^{WT} [37].

In the docked models, larger heterocyclic R_2 groups are shown to interact predominantly with K361 on helix α4 and surrounding residues, a finding corroborated by lowered acylation of a tPBP2^{H041}-K361E mutant by cefoperazone and ceftriaxone. This contrasts with the crystal structure of tPBP2^{WT} acylated by ceftriaxone with the C3 leaving group intact, which shows R_2 interacting with two tyrosine residues on the loop prior to α11 rather than with K361 [42]. Surprisingly, very few poses from our docking studies adopt this conformation. One interesting exception is ceftobiprole, and its R_2 group occupies a position is similar to that observed in the structure of *S. aureus* PBP2a in complex with the same antibiotic [51]. These differences may indicate a difference in binding mode between PBP2^{WT} and PBP2^{H041}, or suggest that a rearrangement of the cephalosporin occurs during the acylation reaction.

Correlations between acylation rate and antimicrobial activity.

Correlation between antimicrobial activity and their second-order rates of acylation was observed for some cephalosporins. For example, cefoperazone and ceftriaxone, which acylate tPBP2^{H041} at relatively high rates, exhibited the most potent antimicrobial activity, while cefaclor, cefsulodin, cephalexin, and cephalothin, which do not acylate tPBP2^{H041}, exhibited the least. Several cephalosporins, however, had poor correlation, which we suspect is due to MICs also reflecting the capacity of an individual ESC to traverse the outer membrane porins or to be expelled by efflux pumps. As a multidrug-resistant pathogen, *N. gonorrhoeae* H041 contains a PorB$_{1B}$ mutant that reduces permeability of the outer membrane [30, 52] and a promoter mutation that overexpresses the *mtrCDE* efflux system [31]. Interestingly, it appears that the same amphipathic features of cephalosporins that favor rapid acylation of tPBP2^{H041} (*i.e.,* large, lipophilic R$_1$ and polar R$_2$) can result in decreased diffusion through porins and increased efflux [53–54]. Examples of cephalosporins that appear to be susceptible to such mechanisms include ceftaroline and ceftobiprole, whose rapid acylation rates contrast with relatively weak antimicrobial potency. This is especially the case for ceftaroline, which is relatively hydrophobic compared to other cephalosporins (logD$_{7.4}$ = 1.03) [55]. The picture is less clear for ceftobiprole, whose relative hydrophilicity (logD$_{7.4}$ = −2.33) suggests it less likely to be removed by efflux pumps. However, MtrCDE also confers resistance to a number of cationic species and may also transport ceftobiprole [56]. Strategic addition of anionic groups to cephalosporins exhibiting rapid tPBP2^{H041} acylation may therefore increase antimicrobial activity by minimizing efflux mechanisms.

Another potential reason for the weak correlation between k_2/K_s and antimicrobial activity is that some cephalosporins may acylate PBP1 more readily than PBP2^{H041}. For example, cefdinir and cefoxitin exhibit very low acylation rates versus tPBP2^{H041}, but relatively high antimicrobial activity with H041 (MICs are 1.5 and 3 μg/mL, respectively), consistent with these antibiotics targeting PBP1 rather than PBP2. In fact, cefdinir and cefoxitin generally show preferential binding to class A and class C PBPs from a number of bacterial species [57–64], and early studies of PBPs from *N. gonorrhoeae* show that cefoxitin acylates PBP1 more rapidly than PBP2 in penicillin-susceptible and –resistant strains [65].

The potential of cefoperazone to treat ESC-resistant gonorrhea.

This work has revealed the third-generation cephalosporin cefoperazone is nearly 7-fold more active against tPBP2^{H041} than ceftriaxone, is comparably potent against the H041 strain, and performs similarly in a mouse model of infection. These findings are consistent with previous studies of gonococcal PBPs that showed cefoperazone bound to (non-mosaic) PBP2 in membrane preparations at concentrations of less than 10^{-3} μg/mL [65], and the fact that cefoperazone has been reported as being highly effective against infections by both penicillin-susceptible and -resistant gonococci [66–68]. In particular, its higher activity against H041 suggests that cefoperazone can overcome, to a large degree, mutations present in PBP2 that confer resistance to ceftriaxone. Cefoperazone is FDA-approved and safe for use in most patients, with tolerated daily doses up to multiple grams and a side effect profile similar to other β-lactam antimicrobials [69]. While the pharmacokinetics (PK) of cefoperazone may be less favorable than ceftriaxone, with a t$_{1/2}$ of 1–2 hours (versus 6–8 hours for ceftriaxone) and primarily biliary excretion (versus primarily renal for CRO) [70],

it may have utility in the treatment of mucosal infections due to its relative lipophilicity. Guided by an appropriate PK study in mice, an optimized dosing strategy could therefore be developed for cefoperazone to take advantage of its higher activity against the target, thus offering a new clinical option for highly resistant gonococcal infections in a relatively barren therapeutic landscape.

In conclusion, the overall picture emerging from our studies is that rapid tPBP2[H041] acylation is promoted by a large R_1 (C7 acylamino side chain) with modestly lipophilic properties, and an electronegative R_2 (C3 side chain) with a planar structure. Unfortunately, these properties may render cephalosporins less permeable to the Gram-negative outer membrane and more prone to efflux, but strategic placement of anionic groups could help to overcome these barriers. Finally, we have shown that cefoperazone holds promise as an antigonococcal agent for strains harboring mosaic *penA* alleles.

Methods

Materials.

The following cephalosporins were kindly provided by Basilea (ceftobiprole), Merck (ceftolozane), and Allergan (ceftaroline). Other cephalosporins were purchased from TCI America Inc, Sigma Aldrich Inc, or Alfa Aesar Inc. The cloning and purification of a C-terminal domain transpeptidase construct of PBP2 derived from the ESC-resistant H041 strain of *N. gonorrhoeae*, termed tPBP2[H041], has been described previously [37]. This construct expresses the transpeptidase domain of PBP2 (237-582) but omits residues 283-297 and joins residues 282 and 298 with a linking glycine. This protein construct is acylated by the fluorescent penicillin Bocillin-FL [71] at the same rate as the full-length protein [72], showing that omission of the N-terminal domain of the protein does not affect the kinetics of acylation for β-lactams. After purification, the protein was dialyzed into Tris-HCl buffer, pH 7.1, with 10 % v/v glycerol and 150 mM NaCl, concentrated to 10-15 mg/ml, and stored in aliquots at −80 °C.

Pharmacophore-constrained docking protocol.

Coordinates for the crystal structure of tPBP2[H041] (PDB ID 6VBC [37]) were prepared by protonation at pH 7.4, explicit solvation with water, and energy minimization against the AMBER forcefield [73] The minimized structure was then allowed to relax with a short (1 ns) molecular dynamics simulation at 2 fs resolution using the NPA algorithm [74]. A pharmacophore model was then generated to constrain the β-lactam ring to the area surrounding the serine nucleophile Ser310, including the oxyanion hole formed by the amide nitrogens of Ser310 and Thr500. Each cephalosporin was flexibly docked with PBP2 using an induced-fit protocol in which compounds were first placed in the fixed active site using the pharmacophore and then scored using the London dG algorithm. The top 50 scored conformers were flexibly refined against the AMBER forcefield where side chains in the PBP2 active site were allowed to rotate and rescored using the GBVI/WSA dG algorithm [75]. Ten rescored conformers were retained for analysis by energy score amplitude, as well as for protein-ligand interaction fingerprint (PLIF) analysis. All modeling calculations were performed using MOE 2018.01 [76].

Determination of second-order acylation rates.

The second-order rate of acylation with Bocillin-FL was determined by time-course kinetic experiments in which 1 μM protein was incubated with 10 to 60 μM Bocillin-FL in 50 mM phosphate-buffered saline (PBS) pH 8.0 at room temperature. Aliquots were removed at specified time points between 2 sec and 1 hr, and the reaction quenched by 4X SDS-PAGE sample buffer. Samples were heated at 95°C for 2 minutes, and acylated protein was separated from free Bocillin-FL using 12% Mini-Protean TGX SDS-PAGE gels. Gels were scanned using a Kodak EDAS 290 UV imaging system, followed by staining with Coomassie R-250 to confirm equal protein loading. Bocillin-FL-bound tPBP2[H041] was quantified by densitometry using ImageJ [77]. Data were normalized to the maximum fluorescence intensity and fit to a one-phase association curve to obtain pseudo-first order rate constants. These were plotted against Bocillin-FL concentration and fit by linear regression to a straight line whose slope was the second-order acylation rate (Figure S4).

Acylation rates for each cephalosporin were then derived by determining the concentration of antibiotic required to inhibit the binding of a specific amount of Bocillin-FL by 50%. tPBP2[H041] (1 μM) was mixed simultaneously with Bocillin-FL (10 or 100 μM) and increasing concentrations (1 μM to 1 mM) of the cephalosporin being tested in 50 mM PBS pH 8.0, followed by 1 hr incubation at room temperature. The reaction was quenched by adding 4X SDS-PAGE sample buffer, the samples were heated at 95°C for 2 min, and then acylated protein was separated from free Bocillin-FL using SDS-PAGE gels and scanned as above. Data were normalized to the maximum fluorescence intensity and fit to a four-parameter inhibitor-response curve to determine half-maximal inhibitory concentrations. An example for ceftriaxone is shown in Figure S11. The acylation rates of the cephalosporins were then determined by the following relationship:

$$k_2/K_s(BOC) \cdot [BOC] = k_2/K_s(Ceph) \cdot IC_{50}(Ceph)$$

where k_2/K_s (BOC) is the acylation rate of Bocillin-FL, [BOC] is the concentration of Bocillin-FL used in the competition experiment, k_2/K_s (Ceph) is the acylation rate of cephalosporin, and IC_{50} (Ceph) is the half-maximal inhibitory concentration of cephalosporin.

Minimal inhibitory concentrations (MIC).

Neisseria gonorrhoeae H041 was passaged on gonococcal medium base (GCB) plates and resuspended at an OD_{600} of 0.018. Four ml of GCB agar was added to the wells of a 24-well plate containing 2-fold changes in concentrations of each cephalosporin and the agar was quickly mixed with a paddle before allowing the agar to solidify. The plates were poured on the day of the experiment. Five microliters of the resuspended cells comprising ~50,000 colony-forming units (CFU) were spotted onto the agar in each well and the plates were incubated overnight. Growth was scored after 24 hr, with growth defined as >5 colonies growing in the spot. The MIC determinations were repeated a minimum of three times, and the values were averaged [78].

Quantitative-structure activity relationship (QSAR).

Partial least squares (PLS) analysis was used to examine the relationship between log-transformed second order acylation rate, $\log(k_2/K_s)$, and molecular descriptor variables for the cephalosporins tested using MOE [76]. Using the knowledge gained from prior crystallographic studies that the regions of the PBP2 active site occupied by the R_1 and R_2 groups are structurally distinct, we separated the descriptors for this model by side chain. The analysis yielded the following linear model:

$$PRED\_log\left(\frac{k_2}{K_s}\right) = \sum_{i=1}^{n} d_i D_i$$

where PRED_log(k_2/K_s) is the predicted second-order acylation rate for a given compound, d_i is the calculated coefficient for the descriptor i, and D_i is the value of descriptor i for the examined compound. Molecular descriptors selected for the QSAR model, as well as their coefficients and normalized weights, are shown in Table 2. Definitions of descriptors used are provided in Table S3. The generated PLS model was validated using the square of the correlation coefficient obtained by the "leave-one-out" cross-validation method. The resulting model was also validated using y-randomization, and by applying to a small test set of cephalosporins.

To examine the relationship between the MIC and molecular descriptors, we also applied a PLS QSAR method except that whole-molecule descriptors were utilized, rather than the side-chain descriptors used to analyze the second-order rates of acylation. The molecular descriptors used for the QSAR and their weights are shown in Table 3. Cefdinir consistently modeled as an outlier, as it exhibits a low rate of PBP2 acylation and yet has high antimicrobial potency, and likely has a different mechanism of action (*e.g.,* it acylates PBP1 rather than PBP2). For this reason, it was excluded from the model. The generated PLS model was validated using the "leave-one-out" cross-validation method, as well as by y-randomization. All analyses, including descriptor calculations and model generation for the PLS analyses, were conducted in MOE 2018.01 [76].

Site directed mutagenesis of tPBP2[H041].

A K361E mutation of tPBP2[H041] was made using the QuikChange Lightning Kit (Agilent, Santa Clara, CA) using the following primers: forward 5'-CATTATGCAAGAATCTTCCAACGTCG-3' and reverse 5'-CCGCGCACATCCAAAGTA-3'. The amplified PCR product was treated with Dpn1 enzyme and then used to transform in *E. coli* BL21 (DE3) cells. The mutation was confirmed by sequencing and the protein (tPBP2[H041]-K361E) was expressed and purified in the same way as for tPBP2[H041] [37].

In vivo evaluation of cefoperazone in a murine model of gonococcal infection.

N. gonorrhoeae strain H041 [35] was made streptomycin resistant for use in the mouse model via allelic replacement of the *rpsL* sequence of FA1090 [39]. Female BALB/c mice (NCI BALB/c strain; 6 to 7 weeks old; Charles River Laboratories) in the diestrus or

anestrus stages of the estrous cycle were implanted with a 5-mg, 21-day-slow-release 17β-estradiol pellet (Innovative Research of America) and treated with antibiotics to promote long-term gonococcal infection per a standard infection protocol [79]. Fifty-five mice were vaginally inoculated with 20 μL H041 (1.6×10^4 CFU/mouse) two days following after pellet implantation and vaginal swabs were cultured for *N. gonorrhoeae* on the following 2 consecutive days to confirm infection. Antibiotic treatment began following the second culture. Stocks of cefoperazone (12, 6 and 2 mg/mL), ceftriaxone (6 mg/mL) and gentamicin (4.8 mg/mL) were prepared at the time of treatment and solubilized in endotoxin-free water (Teknova). The two cephalosporins and the vehicle were administered by intraperitoneal injection at a volume of 10 mL/kg/dose using a TID regimen consisting of three total doses on one day, 8 hours apart). Gentamicin (positive control) was administered once daily for 5 days [39]. Vaginal swabs were quantitatively cultured daily for 8 consecutive days after treatment initiation on GC-VCNTS agar using the Autoplater automated plating system (Spiral Biotech). The number of viable bacteria recovered was determined using the Spiral Biotech Q-Counter Software. The limit of detection for gonococci was 20 CFU/ml; a value of 20 was used in the data analysis for cultures from which no gonococci were recovered. Mice that were culture negative for at least three consecutive days were considered to have cleared H041 infection. Differences in the duration of colonization after initiation of treatment were assessed using a Kaplan Meier survivorship curve and log-rank (Mantel-Cox) test (GraphPad Prism V.7.01). Differences in colonization load were assessed by a repeated measures 2-way ANOVA using Bonferroni as a post hoc analysis for multiple pair wise comparisons (GraphPad Prism V.7.01).

Mice were euthanized using compressed CO_2 gas in the Laboratory Animal Medicine Facility performed under the 2013 AVMA Guidelines on Euthanasia. All work was performed under an approved protocol of the USUHS Institutional Animal Care and Use Committee.

Supplementary Material

Refer to Web version on PubMed Central for supplementary material.

Acknowledgements

Abbreviations

ATAO	2-(2-aminothiazol-4-yl)-2-(alkoxyimino)acetyl
ESC	extended-spectrum cephalosporin
MIC	minimal inhibitory concentration

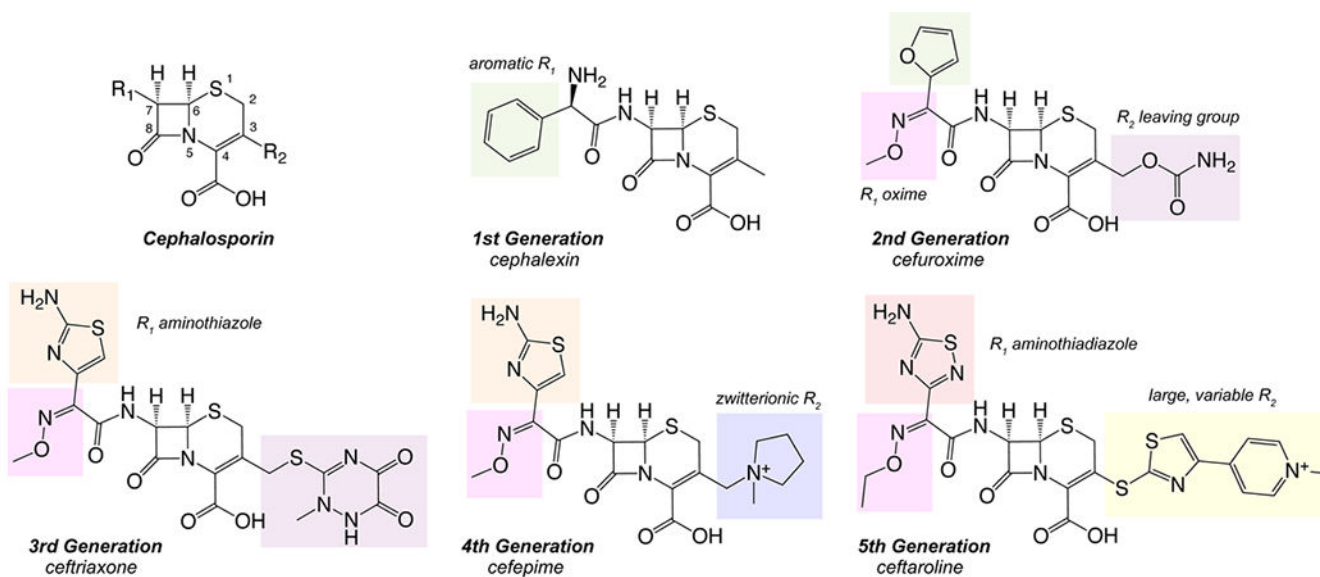| PLIF	protein-ligand interaction fingerprint
PBP	penicillin-binding protein
QIDP	qualified infectious disease product
TID	three-times daily
CFU	colony-forming units

References

1. Satterwhite CL; Torrone E; Meites E; Dunne EF; Mahajan R; Ocfemia MC; Su J; Xu F; Weinstock H, Sexually transmitted infections among US women and men: prevalence and incidence estimates, 2008. Sex Transm Dis 2013, 40, 187–193. [PubMed: 23403598]

2. Newman L; Rowley J; Vander Hoorn S; Wijesooriya NS; Unemo M; Low N; Stevens G; Gottlieb S; Kiarie J; Temmerman M, Global Estimates of the Prevalence and Incidence of Four Curable Sexually Transmitted Infections in 2012 Based on Systematic Review and Global Reporting. PLoS One 2015, 10, e0143304. [PubMed: 26646541]

3. Piszczek J; St Jean R; Khaliq Y, Gonorrhea: Treatment update for an increasingly resistant organism. Can Pharm J (Ott) 2015, 148, 82–89. [PubMed: 25918540]

4. Wasserheit JN, Epidemiological synergy. Interrelationships between human immunodeficiency virus infection and other sexually transmitted diseases. Sex. Transm. Dis 1992, 19, 61–77. [PubMed: 1595015]

5. Akasaka S; Muratani T; Yamada Y; Inatomi H; Takahashi K; Matsumoto T, Emergence of cephem- and aztreonam-high-resistant Neisseria gonorrhoeae that does not produce beta-lactamase. J. Infect. Chemother 2001, 7, 49–50. [PubMed: 11406757]

6. Muratani T; Akasaka S; Kobayashi T; Yamada Y; Inatomi H; Takahashi K; Matsumoto T, Outbreak of cefozopran (penicillin, oral cephems, and aztreonam)-resistant Neisseria gonorrhoeae in Japan. Antimicrob. Agents Chemother 2001, 45, 3603–3606. [PubMed: 11709349]

7. Ito M; Deguchi T; Mizutani KS; Yasuda M; Yokoi S; Ito S; Takahashi Y; Ishihara S; Kawamura Y; Ezaki T, Emergence and spread of Neisseria gonorrhoeae clinical isolates harboring mosaic-like structure of penicillin-binding protein 2 in Central Japan. Antimicrob. Agents Chemother 2005, 49, 137–143. [PubMed: 15616287]

8. Lindberg R; Fredlund H; Nicholas R; Unemo M, Neisseria gonorrhoeae isolates with reduced susceptibility to cefixime and ceftriaxone: association with genetic polymorphisms in penA, mtrR, porB1b, and ponA. Antimicrob Agents Chemother 2007, 51, 2117–2122. [PubMed: 17420216]

9. Ohnishi M; Saika T; Hoshina S; Iwasaku K; Nakayama S; Watanabe H; Kitawaki J, Ceftriaxone-resistant Neisseria gonorrhoeae, Japan. Emerg Infect Dis 2011, 17, 148–149. [PubMed: 21192886]

10. Unemo M; Golparian D; Nicholas R; Ohnishi M; Gallay A; Sednaoui P, High-level cefixime- and ceftriaxone-resistant Neisseria gonorrhoeae in France: novel penA mosaic allele in a successful international clone causes treatment failure. Antimicrob Agents Chemother 2012, 56, 1273–1280. [PubMed: 22155830]

11. Camara J; Serra J; Ayats J; Bastida T; Carnicer-Pont D; Andreu A; Ardanuy C, Molecular characterization of two high-level ceftriaxone-resistant Neisseria gonorrhoeae isolates detected in Catalonia, Spain. J Antimicrob Chemother 2012, 67, 1858–1860. [PubMed: 22566592]

12. Tapsall J; Read P; Carmody C; Bourne C; Ray S; Limnios A; Sloots T; Whiley D, Two cases of failed ceftriaxone treatment in pharyngeal gonorrhoea verified by molecular microbiological methods. J Med Microbiol 2009, 58, 683–687. [PubMed: 19369534]

13. Unemo M; Golparian D; Syversen G; Vestrheim DF; Moi H, Two cases of verified clinical failures using internationally recommended first-line cefixime for gonorrhoea treatment, Norway, 2010. Euro Surveill. 2010, 15, pii: 19721.

14. Unemo M; Golparian D; Hestner A, Ceftriaxone treatment failure of pharyngeal gonorrhoeae verified by international recommendations, Sweden, July 2010. Euro Surveill. 2011, 16, 1–3.

15. Ison CA; Hussey J; Sankar KN; Evans J; Alexander S, Gonorrhoea treatment failures to cefixime and azithromycin in England, 2010. Euro Surveill 2011, 16, 19833. [PubMed: 21492528]

16. Workowski KA; Bolan GA; Centers for Disease C; Prevention, Sexually transmitted diseases treatment guidelines, 2015. MMWR Recomm Rep 2015, 64, 1–137.

17. Unemo M; Lahra MM; Cole M; Galarza P; Ndowa F; Martin I; Dillon JR; Ramon-Pardo P; Bolan G; Wi T, World Health Organization Global Gonococcal Antimicrobial Surveillance Program (WHO GASP): review of new data and evidence to inform international collaborative actions and research efforts. Sex Health 2019, 16, 412–425. [PubMed: 31437420]

18. Bignell C; Unemo M; Board ESTIGE, 2012 European guideline on the diagnosis and treatment of gonorrhoea in adults. Int J STD AIDS 2013, 24, 85–92. [PubMed: 24400344]

19. Public Health Agency of Canada, Canadian Guidelines on Sexually Transmitted Infections – Management and treatment of specific infections - Gonococcal Infections (2013 (modified Sept 2017). Government of Canada, Ottawa ON: 2013.

20. Eyre DW; Sanderson ND; Lord E; Regisford-Reimmer N; Chau K; Barker L; Morgan M; Newnham R; Golparian D; Unemo M; Crook DW; Peto TE; Hughes G; Cole MJ; Fifer H; Edwards A; Andersson MI, Gonorrhoea treatment failure caused by a Neisseria gonorrhoeae strain with combined ceftriaxone and high-level azithromycin resistance, England, February 2018. Euro Surveill 2018, 23, 1800323. [PubMed: 29991383]

21. Whiley DM; Jennison A; Pearson J; Lahra MM, Genetic characterisation of Neisseria gonorrhoeae resistant to both ceftriaxone and azithromycin. The Lancet. Infectious diseases 2018, 18, 717–718. [PubMed: 29976521]

22. Macheboeuf P; Contreras-Martel C; Job V; Dideberg O; Dessen A, Penicillin binding proteins: key players in bacterial cell cycle and drug resistance processes. FEMS Microbiol. Rev 2006, 30, 673–691. [PubMed: 16911039]

23. Sauvage E; Kerff F; Terrak M; Ayala JA; Charlier P, The penicillin-binding proteins: structure and role in peptidoglycan biosynthesis. FEMS Microbiol. Rev 2008, 32, 234–258. [PubMed: 18266856]

24. Vollmer W; Blanot D; de Pedro MA, Peptidoglycan structure and architecture. FEMS Microbiol. Rev 2008, 32, 149–167. [PubMed: 18194336]

25. Barbour AG, Properties of penicillin-binding proteins in Neisseria gonorrhoeae. Antimicrob Agents Chemother 1981, 19, 316–322. [PubMed: 6812490]

26. Stefanova ME; Tomberg J; Olesky M; Holtje JV; Gutheil WG; Nicholas RA, Neisseria gonorrhoeae penicillin-binding protein 3 exhibits exceptionally high carboxypeptidase and beta-lactam binding activities. Biochemistry 2003, 42, 14614–14625. [PubMed: 14661974]

27. Goffin C; Ghuysen JM, Multimodular penicillin-binding proteins: an enigmatic family of orthologs and paralogs. Microbiol. Mol. Biol. Rev 1998, 62, 1079–1093. [PubMed: 9841666]

28. Frere JM; Ghuysen JM; Iwatsubo M, Kinetics of interaction between the exocellular DD-carboxypeptidase- transpeptidase from Streptomyces R61 and beta-lactam antibiotics. A choice of models. Eur. J. Biochem 1975, 57, 343–351. [PubMed: 1175647]

29. Frere JM; Joris B, Penicillin-sensitive enzymes in peptidoglycan biosynthesis. Crit Rev Microbiol 1985, 11, 299–396. [PubMed: 3888533]

30. Olesky M; Hobbs M; Nicholas RA, Identification and analysis of amino acid mutations in porin IB that mediate intermediate-level resistance to penicillin and tetracycline in Neisseria gonorrhoeae. Antimicrob Agents Chemother 2002, 46, 2811–2820. [PubMed: 12183233]

31. Veal WL; Nicholas RA; Shafer WM, Overexpression of the MtrC-MtrD-MtrE efflux pump due to an mtrR mutation is required for chromosomally mediated penicillin resistance in Neisseria gonorrhoeae. J. Bacteriol 2002, 184, 5619–5624. [PubMed: 12270819]

32. Ropp PA; Hu M; Olesky M; Nicholas RA, Mutations in ponA, the gene encoding penicillin-binding protein 1, and a novel locus, penC, are required for high-level chromosomally mediated penicillin resistance in Neisseria gonorrhoeae. Antimicrob Agents Chemother 2002, 46, 769–777. [PubMed: 11850260]

33. Brannigan JA; Tirodimos IA; Zhang QY; Dowson CG; Spratt BG, Insertion of an extra amino acid is the main cause of the low affinity of penicillin-binding protein 2 in penicillin-resistant strains of Neisseria gonorrhoeae. Mol. Microbiol 1990, 4, 913–919. [PubMed: 2120542]

34. Whiley DM; Limnios EA; Ray S; Sloots TP; Tapsall JW, Diversity of penA alterations and subtypes in Neisseria gonorrhoeae strains from Sydney, Australia, that are less susceptible to ceftriaxone. Antimicrob. Agents Chemother 2007, 51, 3111–3116. [PubMed: 17591846]

35. Ohnishi M; Golparian D; Shimuta K; Saika T; Hoshina S; Iwasaku K; Nakayama S; Kitawaki J; Unemo M, Is Neisseria gonorrhoeae initiating a future era of untreatable gonorrhea?: detailed characterization of the first strain with high-level resistance to ceftriaxone. Antimicrob Agents Chemother 2011, 55, 3538–3545. [PubMed: 21576437]

36. Tomberg J; Unemo M; Ohnishi M; Davies C; Nicholas RA, Identification of amino acids conferring high-level resistance to expanded-spectrum cephalosporins in the penA gene from Neisseria gonorrhoeae strain H041. Antimicrob Agents Chemother 2013, 57, 3029–3036. [PubMed: 23587946]

37. Singh A; Turner JM; Tomberg J; Fedarovich A; Unemo M; Nicholas RA; Davies C, Mutations in penicillin-binding protein 2 from cephalosporin-resistant Neisseria gonorrhoeae hinder ceftriaxone acylation by restricting protein dynamics. J Biol Chem 2020, 295, 7529–7543. [PubMed: 32253235]

38. Ghuysen JM; Frere JM; Leyh-Bouille M; Coyette J; Dusart J; Nguyen-Disteche M, Use of model enzymes in the determination of the mode of action of penicillins and delta 3-cephalosporins. Ann. Rev. Biochem 1979, 48, 73–101. [PubMed: 112913]

39. Connolly KL; Eakin AE; Gomez C; Osborn BL; Unemo M; Jerse AE, Pharmacokinetic Data Are Predictive of In Vivo Efficacy for Cefixime and Ceftriaxone against Susceptible and Resistant Neisseria gonorrhoeae Strains in the Gonorrhea Mouse Model. Antimicrob. Agents Chemother 2019, 63, e01644–18. [PubMed: 30642924]

40. Jerse AE; Wu H; Packiam M; Vonck RA; Begum AA; Garvin LE, Estradiol-Treated Female Mice as Surrogate Hosts for Neisseria gonorrhoeae Genital Tract Infections. Front. Microbiol 2011, 2, 107. [PubMed: 21747807]

41. Hujer AM; Kania M; Gerken T; Anderson VE; Buynak JD; Ge X; Caspers P; Page MG; Rice LB; Bonomo RA, Structure-activity relationships of different beta-lactam antibiotics against a soluble form of Enterococcus faecium PBP5, a type II bacterial transpeptidase. Antimicrob Agents Chemother 2005, 49, 612–618. [PubMed: 15673741]

42. Singh A; Tomberg J; Nicholas RA; Davies C, Recognition of the beta-lactam carboxylate triggers acylation of Neisseria gonorrhoeae penicillin-binding protein 2. J Biol Chem 2019, 294, 14020–14032. [PubMed: 31362987]

43. Sassiver ML; Lewis A, Structure–Activity Relationships Among Semisynthetic Cephalosporins. Adv. App. Microbiol 1970, 13, 163–236.

44. Flynn EH, Cephalosporins and Penicillins: Chemistry and Biology. Academic Press: New York, NY, 1972.

45. Ochiai M; Aki O; Morimoto A; Okada T; Matsushita Y, New cephalosporin derivatives with high antibacterial activities. Chem Pharm Bull (Tokyo) 1977, 25, 3115–3117. [PubMed: 603968]

46. Reiner R; Weiss U; Brombacher U; Lanz P; Montavon M; Furlenmeier A; Angehrn P; Probst PJ, Ro 13–9904/001, a novel potent and long-acting parenteral cephalosporin. J Antibiot (Tokyo) 1980, 33, 783–786. [PubMed: 6967869]

47. Boyd DB, Electronic structures of cephalosporins and penicillins. 15. Inductive effect of the 3-position side chain in cephalosporins. J. Med. Chem 1984, 27, 63–66. [PubMed: 6690684]

48. Boyd DB; Hermann RB; Presti DE; Marsh MM, Electronic structures of cephalosporins and penicillins. 4. Modeling acylation by the beta-lactam ring. J. Med. Chem 1975, 18, 408–417. [PubMed: 1121009]

49. Pratt RF; Faraci WS, Direct observation by proton NMR of cephalosporoate intermediates in aqueous solution during the hydrazinolysis and beta-lactamase-catalyzed hydrolysis of cephalosporins with 3' leaving groups: kinetics and equilibria of the 3' elimination reaction. J. Am. Chem. Soc 1986, 108, 5328–5333.

50. Faraci WS; Pratt RF, Interactions of cephalosporins with the Streptomyces R61 DD-transpeptidase/carboxypeptidase. Influence of the 3'-substituent. Biochem. J 1986, 238, 309–312. [PubMed: 3800940]

51. Lovering AL; Gretes MC; Safadi SS; Danel F; de Castro L; Page MG; Strynadka NC, Structural insights into the anti-methicillin-resistant Staphylococcus aureus (MRSA) activity of ceftobiprole. J. Biol. Chem 2012, 287, 32096–32102. [PubMed: 22815485]

52. Olesky M; Zhao S; Rosenberg RL; Nicholas RA, Porin-mediated antibiotic resistance in Neisseria gonorrhoeae: ion, solute and antibiotic permation through PIB proteins with penB mutations. J. Bacteriol 2006, 188, 2300–2308. [PubMed: 16547016]

53. Hagman KE; Pan W; Spratt BG; Balthazar JT; Judd RC; Shafer WM, Resistance of Neisseria gonorrhoeae to antimicrobial hydrophobic agents is modulated by the mtrRCDE efflux system. Microbiology 1995, 141, 611–622. [PubMed: 7711899]

54. Hagman KE; Lucas CE; Balthazar JT; Snyder L; Nilles M; Judd RC; Shafer WM, The MtrD protein of Neisseria gonorrhoeae is a member of the resistance/nodulation/division protein family constituting part of an efflux system. Microbiology 1997, 143 2117–2125. [PubMed: 9245801]

55. Lagace-Wiens PRS; Adam HJ; Laing NM; Baxter MR; Martin I; Mulvey MR; Karlowsky JA; Hoban DJ; Zhanel GG, Antimicrobial susceptibility of clinical isolates of Neisseria gonorrhoeae to alternative antimicrobials with therapeutic potential. J Antimicrob Chemother 2017, 72, 2273–2277. [PubMed: 28505331]

56. Shafer WM; Qu X; Waring AJ; Lehrer RI, Modulation of Neisseria gonorrhoeae susceptibility to vertebrate antibacterial peptides due to a member of the resistance/nodulation/division efflux pump family. Proc Natl Acad Sci U S A 1998, 95, 1829–1833. [PubMed: 9465102]

57. Fukuoka T; Ohya S; Utsui Y; Domon H; Takenouchi T; Koga T; Masuda N; Kawada H; Kakuta M; Kubota M; Ishii C; Ishii C; Sakagawa E; Harasaki T; Hirasawa A; Abe T; Yasuda H; Iwata M; Kuwahara S, In vitro and in vivo antibacterial activities of CS-834, a novel oral carbapenem. Antimicrob. Agents Chemother 1997, 41, 2652–2663. [PubMed: 9420035]

58. Inui T; Oshida T; Endo T; Matsushita T, Potent bacteriolytic activity of ritipenem associated with a characteristic profile of affinities for penicillin-binding proteins of Haemophilus influenzae. Antimicrob. Agents Chemother 1999, 43, 2534–2537. [PubMed: 10508039]

59. Watanabe Y; Hatano K; Matsumoto Y; Tawara S; Yamamoto H; Kawabata K; Takasugi H; Matsumoto F; Kuwahara S, In vitro antibacterial activity of FK041, a new orally active cephalosporin. J Antibiot (Tokyo) 1999, 52, 649–659. [PubMed: 10513845]

60. Sakagawa E; Otsuki M; Oh T; Nishino T, In-vitro and in-vivo antibacterial activities of CS-834, a new oral carbapenem. J. Antimicrob. Chemother 1998, 42, 427–437. [PubMed: 9818740]

61. Sharifzadeh S; Dempwolff F; Kearns DB; Carlson EE, Harnessing beta-Lactam Antibiotics for Illumination of the Activity of Penicillin-Binding Proteins in Bacillus subtilis. ACS Chem. Biol 2020, 15, 1242–1251. [PubMed: 32155044]

62. Chambers HF; Sachdeva M, Binding of beta-lactam antibiotics to penicillin-binding proteins in methicillin-resistant Staphylococcus aureus. J Infect Dis 1990, 161, 1170–1176. [PubMed: 2345297]

63. Matsuhashi M; Tamaki S, Enzymatic studies on the mechanism of action of cefoxitin. Correlation between the affinities of cefoxitin to penicillin-binding proteins and its rates of inhibition of the respective penicillin-sensitive reactions in E. coli. J Antibiot (Tokyo) 1978, 31, 1292–1295. [PubMed: 368000]

64. Ohya S; Yamazaki M; Sugawara S; Tamaki S; Matsuhashi M, New cephamycin antibiotic, CS-1170: binding affinity to penicillin-binding proteins and inhibition of peptidoglycan cross-linking reactions in Escherichia coli. Antimicrob. Agents Chemother 1978, 14, 780–785. [PubMed: 365089]

65. Dougherty TJ; Koller AE; Tomasz A, Competition of beta-lactam antibiotics for the penicillin-binding proteins of Neisseria gonorrhoeae. Antimicrob. Agents Chemother 1981, 20, 109–114. [PubMed: 6792979]

66. Kim JH; Ro YS; Kim YT, Cefoperazone (Cefobid) for treating men with gonorrhoea caused by penicillinase producing Neisseria gonorrhoeae. Br J Vener Dis 1984, 60, 238–240. [PubMed: 6430464]

67. Kim JH; Kim YT; Hwang DH, Cefoperazone for urethritis due to penicillinase-producing Neisseria gonorrhoeae. Clin Ther 1984, 6, 193–197. [PubMed: 6423283]

68. Hook EW 3rd; Judson FN; Verdon MS; Ehret JM; Handsfield HH, Comparative study of cefoperazone and spectinomycin for treatment of uncomplicated gonorrhea in men. Antimicrob. Agents Chemother 1986, 30, 619–621. [PubMed: 2947537]

69. Paradisi F; de Crescenzo G; Ruffilli MP, [Multicenter research on cefoperazone efficacy and tolerance in the therapy of urinary and respiratory infections]. Minerva Med 1989, 80, 43–51. [PubMed: 2644585]

70. Craig WA; Gerber AU, Pharmacokinetics of cefoperazone: a review. Drugs 1981, 22 Suppl 1, 35–45. [PubMed: 6456890]

71. Zhao G; Meier TI; Kahl SD; Gee KR; Blaszczak LC, BOCILLIN FL, a sensitive and commercially available reagent for detection of penicillin-binding proteins. Antimicrob. Agents Chemother 1999, 43, 1124–1128. [PubMed: 10223924]

72. Fedarovich A; Cook E; Tomberg J; Nicholas RA; Davies C, Structural effect of the Asp345a insertion in penicillin-binding protein 2 from penicillin-resistant strains of Neisseria gonorrhoeae. Biochemistry 2014, 53, 7596–7603. [PubMed: 25403720]

73. Cornell WD; Cieplak P; Bayly CI; Gould IR; Merz KM; Ferguson DM; Spellmeyer DC; Fox T; Caldwell JW; Kollman PA, A Second Generation Force Field for the Simulation of Proteins, Nucleic Acids, and Organic Molecules. Journal of the American Chemical Society 1995, 117, 5179–5197.

74. Sturgeon JB; Laird BB, Symplectic algorithm for constant-pressure molecular dynamics using a Nosé–Poincaré thermostat. The Journal of Chemical Physics 2000, 112, 3474–3482.

75. Wojciechowski M; Lesyng B, Generalized Born Model: Analysis, Refinement, and Applications to Proteins. The Journal of Physical Chemistry B 2004, 108, 18368–18376.

76. Vilar S; Cozza G; Moro S, Medicinal chemistry and the molecular operating environment (MOE): application of QSAR and molecular docking to drug discovery. Curr Top Med Chem 2008, 8, 1555–1572. [PubMed: 19075767]

77. Schneider CA; Rasband WS; Eliceiri KW, NIH Image to ImageJ: 25 years of image analysis. Nat Methods 2012, 9, 671–675. [PubMed: 22930834]

78. Zhao S; Duncan M; Tomberg J; Davies C; Unemo M; Nicholas RA, Genetics of chromosomally mediated intermediate resistance to ceftriaxone and cefixime in Neisseria gonorrhoeae. Antimicrob. Agents Chemother 2009, 53, 3744–3751. [PubMed: 19528266]

79. Jerse AE; Wu H; Packiam M; Vonck RA; Begum AA; Garvin LE, Estradiol-Treated Female Mice as Surrogate Hosts for Neisseria gonorrhoeae Genital Tract Infections. Frontiers in Microbiology 2011, 2, 107. [PubMed: 21747807]

Figure 1: Generations of cephalosporin antimicrobials.
Representative structures from each generation show new features discovered and adapted during each generation.
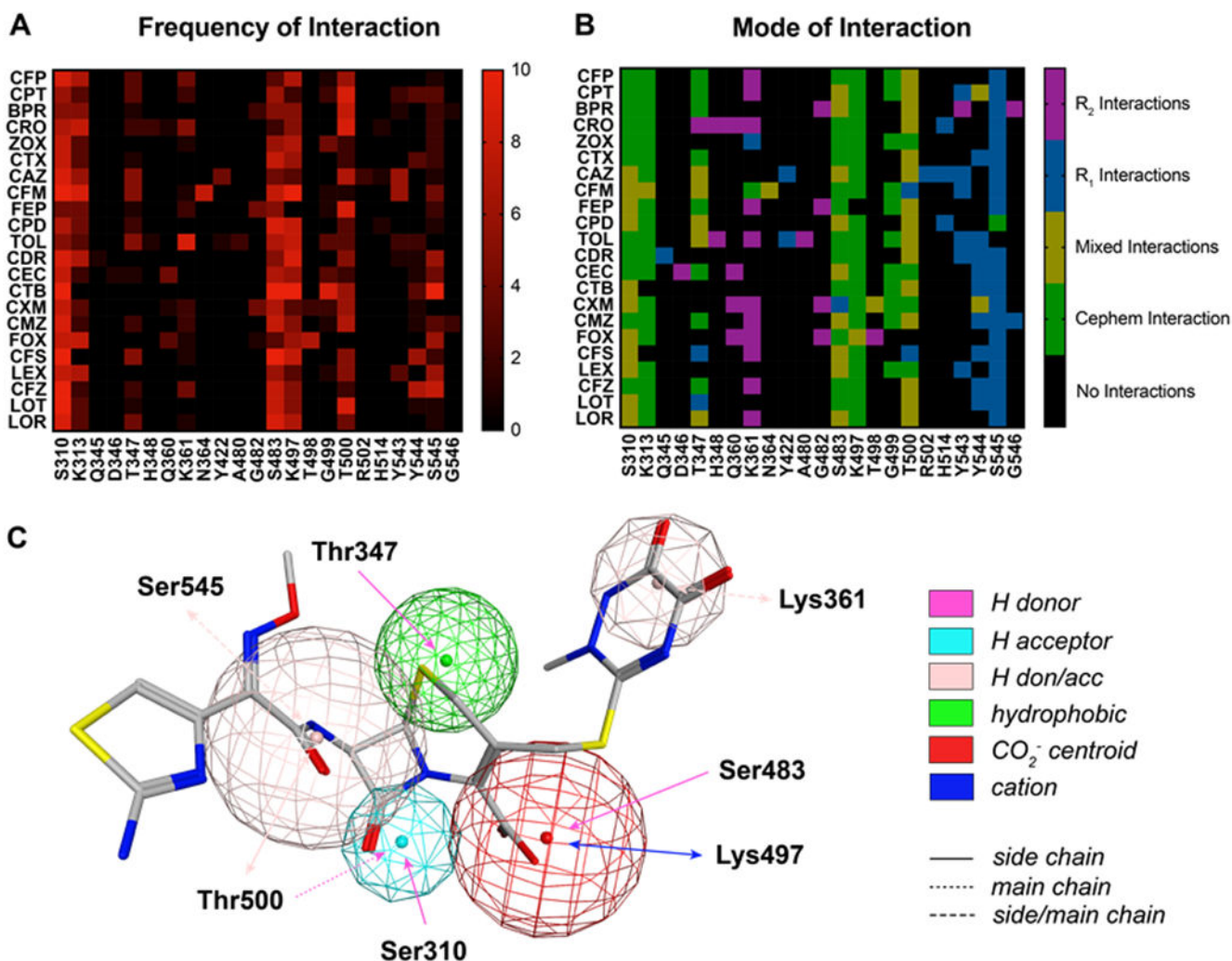
Figure 2: Protein-ligand interaction fingerprints (PLIFs) for pharmacophore-constrained induced-fit docking of cephalosporins to tPBP2^{H041}.
A. Heat map of cephalosporin-tPBP2^{H041} interactions colored by number of poses interacting with a given residue. **B.** Heat map of cephalosporin-tPBP2^{H041} interactions, colored by the cephalosporin moiety interacting with a given residue. **C.** Consensus pharmacophore generated from all docked poses, set against a representative pose of ceftriaxone. The radius of the sphere indicates the variance of a given feature across all poses. Key: cefoperazone (CFP), ceftaroline (CPT), ceftobiprole (BPR), ceftriaxone (CRO, ceftizoximine (ZOX), cefotaxime (CTX), ceftazidime (CAZ), cefixime (CFM), cefepime (FEP), cefpodoxime (CPD), ceftolozane (TOL), cefdinir (CDR), cefaclor (CEC), ceftibuten (CTB), cefuroxime (CXM), cefmetazole (CMZ), cefoxitin (FOX), cefsulodin (CFS), cephalexin (LEX), cefazolin (CFZ), cephalothin (LOT), cephaloridine (LOR).
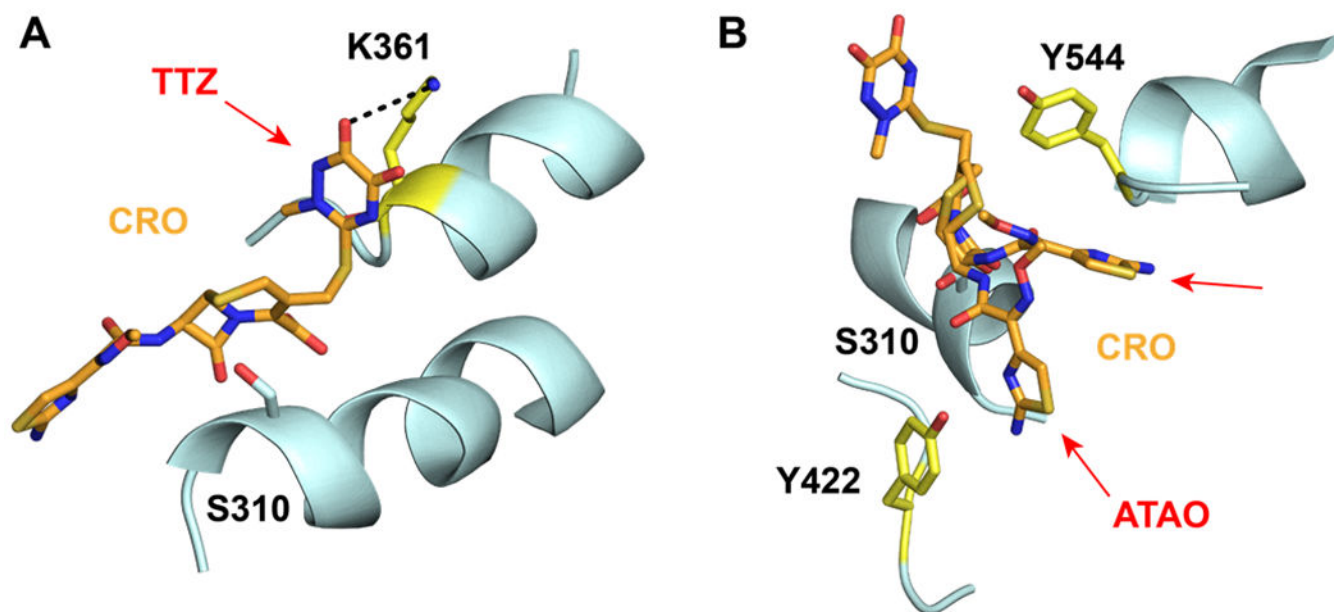
Figure 3: Positioning of the R$_1$ and R$_2$ groups of ceftriaxone within the active site of tPBP2^{H041}.
A. The thiotriazinone (TTZ) R$_2$ of ceftriaxone (CRO, orange) makes contact with K361 (yellow) in a majority of docked poses. The predicted hydrogen bond between TZZ and Lys361 is shown with a dashed line. **B**. The ATAO R$_1$ group of CRO (orange) adopts two conformations in the docked poses. In each conformation, R$_1$ is in close proximity to either Y422 or Y544 (both colored yellow).
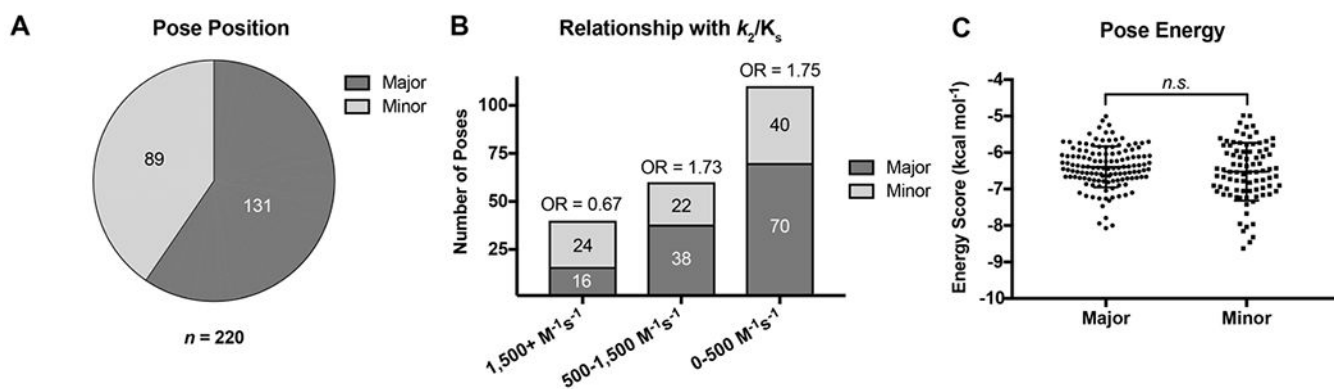
Figure 4: Inspection of individual docked poses reveals two distinct predicted binding modes, representative poses of which are shown in Figure 5 and Figure S2.

A. Pie chart showing the relative abundance of the two predicted binding modes. **B.** Predicted binding mode abundance stratified by second-order acylation rate constant. **C.** Pooled energy scores for poses in each of the two predicted binding modes.
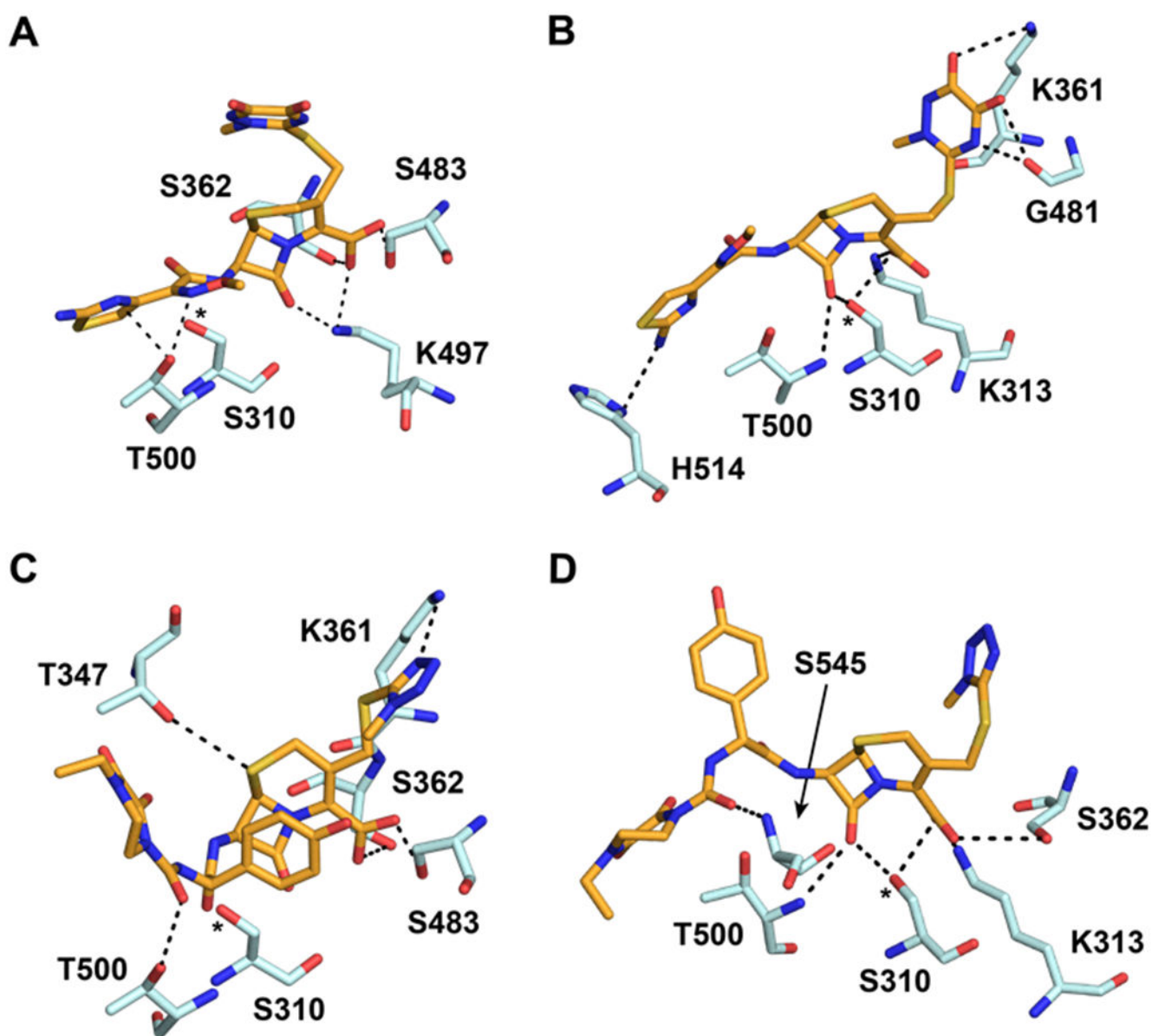
Figure 5: Representative poses of ceftriaxone and cefoperazone.
A. In the major pose predicted by the pharmacophore-constrained docking protocol, the C4 carboxylate of ceftriaxone interacts with S483, its R_2 side chain interacts with K361, and the β-lactam ring system is not optimally oriented for nucleophilic attack by S310. **B.** In the minor pose, the C4 carboxylate interacts with the side chains of K313 and S310, and the β-lactam ring is available for attack by S310. **C.** Cefoperazone in the major pose. **D.** CFP in the minor pose. For all panels, ceftriaxone (CRO) and cefoperazone (CFP) are shown with orange bonds, and potential hydrogen bonds made involving the antibiotic are indicated by dashed lines. *Nucleophilic Oγ of S310.
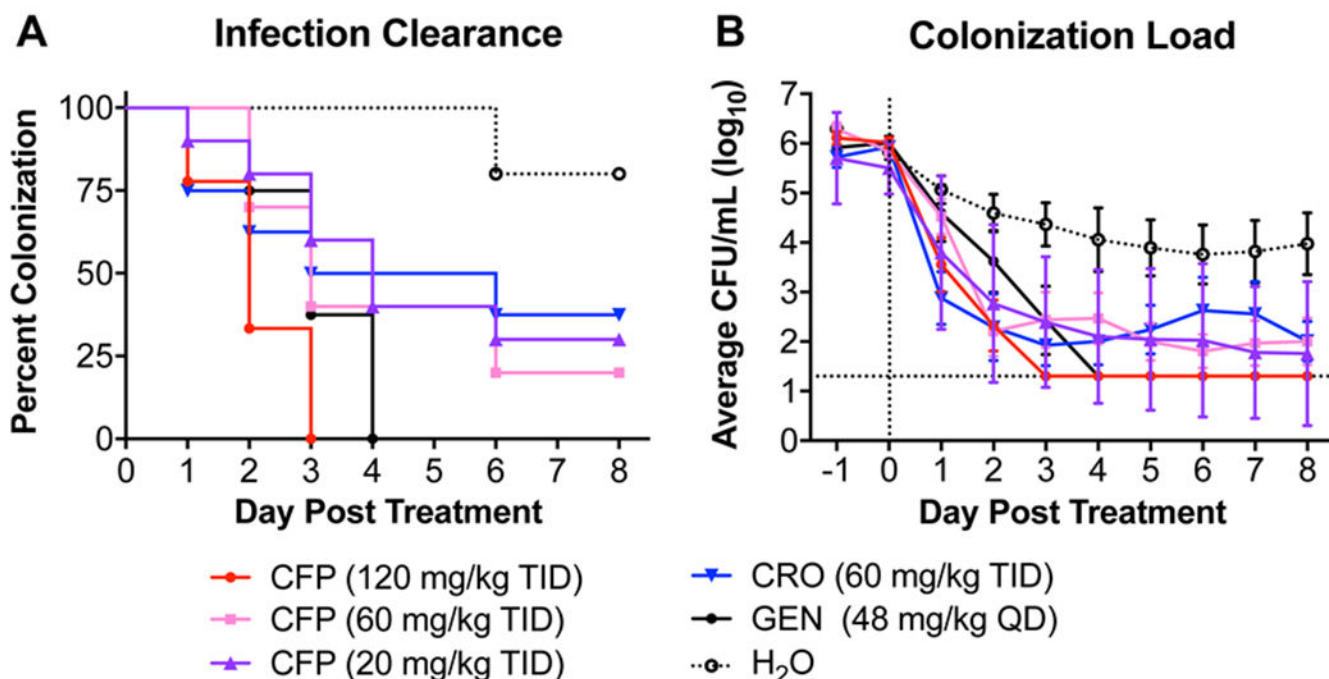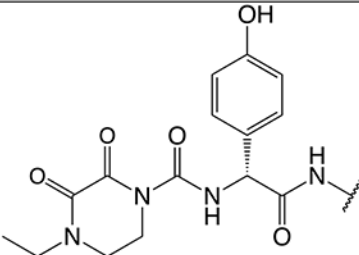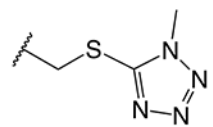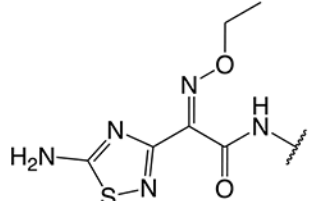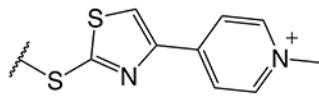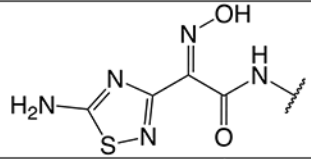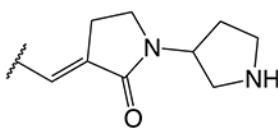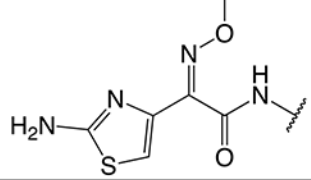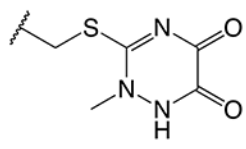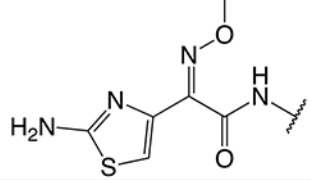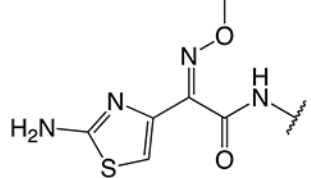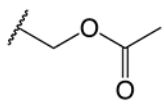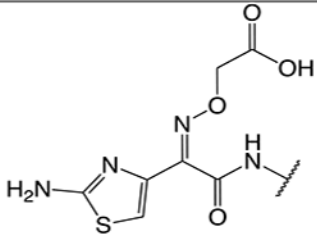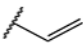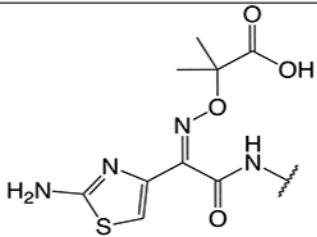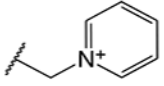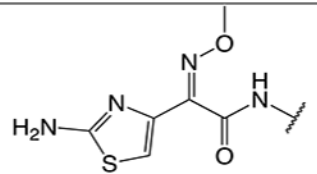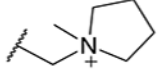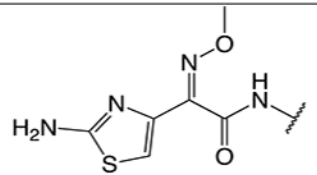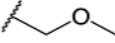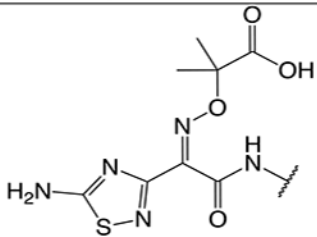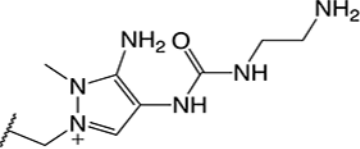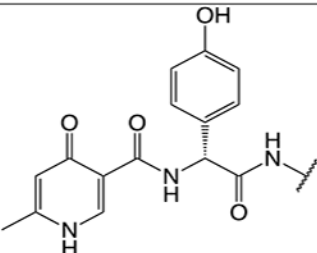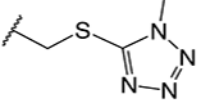
Figure 6: Evaluation of decreasing doses of cefoperazone given three-times daily (TID) on one day in a murine model of gonococcal infection.

Mice were infected with *N. gonorrhoeae* strain H041 two days prior to treatment. Treatments began on day 0 and were cefoperazone (CFP), ceftriaxone (CRO) (comparator control), water (vehicle control), or gentamicin (GEN) (positive control). Each color represents a given treatment group as described in the legend. **A.** Percent of infected mice following administration of CFP. Differences were analyzed by the Log-rank (Mantel-Cox) test comparing all treatment and control groups. Mice that were culture negative (no H041 recovered) for 3 or more days were considered to have cleared infection. A significant Log-rank test for trend of CFP treatments indicated a dose response was observed. **B.** Bacterial burden recovered from each experimental group following administration of CFP. Data points are the average CFU/mL of vaginal swab suspension (log transformed) recovered from each group. Error bars indicate the standard error of the mean. The limit of detection (20 CFU) is denoted with a horizontal dashed line. For mice that had no recoverable CFU, a value of 20 was entered for analysis. Differences were compared by 2-way ANOVA with repeated measures with Bonferroni post-hoc analysis used for multiple comparisons.

Table 1:

Second-order acylation rates and minimum inhibitory concentrations for the selected panel of cephalosporins.

Cephalosporin	R₁	R₂	k_2/K_s $(M^{-1}s^{-1})^a$	median MIC $(\mu g/mL)^b$ [range]
cefoperazone (CFP)			11,800 ± 1,300	1 [1]
ceftaroline (CPT)			10,900 ± 1,700	2 [1-4]
ceftobiprole (BPR)			3,230 ± 190	4 [2-4]
ceftriaxone (CRO)			1,710 ± 320	2 [1-4]
ceftizoxime (ZOX)		H	1,000 ± 210	6 [4-8]
cefotaxime (CTX)			880 ± 120	6 [4-8]

cefixime (CFM)			720 ± 60	6 [4-8]
ceftazidime (CAZ)			790 ± 150	24 [16-32]
cefepime (FEP)			630 ± 50	32 [16-32]
cefpodoxime (CPD)			590 ± 90	16 [16]
ceftolozane (TOL)			200 ± 20	>32
cefpiramide (CPM)			120 ± 14	ND

Compound	R1 structure	R2 structure	k_2/K_S	MIC
cefdinir (CDR)			82 ± 7	1.5 [1-2]
cefaclor (CEC)		Cl	29 ± 4	>32
ceftibuten (CTB)		H	19.1 ± 0.2	>32
cefuroxime (CXM)			6.8 ± 0.2	16 [16]
cefoxitin (FOX)			3.3 ± 0.6	3 [2-4]
cefmetazole (CMZ)			3.6 ± 0.1	32 [32]
cefsulodin (CFS)			0.8 ± 0.1	>32
cephalexin (LEX)		CH₃	~ 0.3[†]	>32
cefazolin (CFZ)			~ 0[‡]	12 [8-16]
cephalothin (LOT)			~ 0[‡]	32 [32]
cephaloridine (LOR)			~ 0[‡]	16 [16]

[a]The acylation rate constant (k_2/K_S) for each cephalosporin was derived from kinetic measurements of the formation of the acyl-enzyme complex using a competition assay, as described in Methods. Values were derived from a minimum of three separate determinations.

[b]The minimum inhibitory concentration (MIC) for each cephalosporin was determined against *N. gonorrhoeae* H041 using an agar dilution protocol, as described in Methods. Values were derived from a minimum of three separate determinations.

[†]Inhibition plot could not be fit due to lack of a plateau at the highest concentration used; however, approximately 50% inhibition was seen at 10 mM.

[‡]Inhibition plot could not be fit due to minimal inhibition seen at the highest concentration used.

Table 2:

Partial least squares QSAR model of tPBP2^{H041} acylation rate constant data.

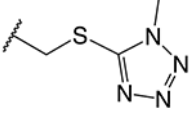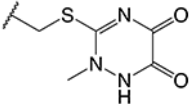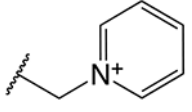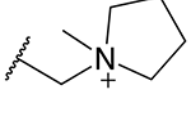| Descriptor	Moiety	Coefficient	Importance
vdw_area	R$_1$	+ 4.8926	1
Kier1	R$_1$	− 4.5005	0.9198
zagreb	R$_1$	− 0.8829	0.1804
KierA2	R$_1$	+ 0.6690	0.1367
chi0v	R$_1$	+ 0.5917	0.1209
BCUT_SLOGP_0	R$_1$	− 0.5145	0.1052
BCUT_SLOGP_1	R$_1$	− 0.3783	0.0773
a_ICM	R$_1$	+ 0.3723	0.0761
SlogP_VSA7	R$_2$	+ 0.3679	0.0752
BCUT_SLOGP_3	R$_1$	− 0.3626	0.0741
BCUT_SMR_3	R$_1$	− 0.1991	0.0407
a_acc	R$_2$	+ 0.1939	0.0396
BCUT_PEOE_3	R$_1$	− 0.1797	0.0367
GCUT_PEOE_2	R$_2$	+ 0.1737	0.0355
BCUT_PEOE_0	R$_1$	+ 0.1693	0.0346
PEOE_VSA_FPNEG	R$_1$	+ 0.1104	0.0226
Q_RPC+	R$_2$	+ 0.0854	0.0175

[a]Descriptor definitions can be found in Table S3.

Table 3:

Partial least squares QSAR model of Neisseria gonorrhoeae antimicrobial activity data.

Descriptor	Coefficient	Importance
KierFlex	−2.21534	1
SlogP_VSA1	1.9259	0.869347
a_donacc	1.83183	0.826884
SlogP_VSA0	−1.48259	0.669238
PEOE_VSA-4	1.477	0.666712
PEOE_VSA+3	1.35739	0.612723
PEOE_VSA-1	1.08015	0.487576
Q_VSA_HYD	−0.75623	0.341362
zagreb	−0.74312	0.335441
SlogP_VSA4	−0.73469	0.331639
h_logS	0.69732	0.314768
PEOE_VSA+1	0.68026	0.307066
chi1v_C	0.65965	0.297765
PEOE_VSA+0	0.56833	0.256542
SlogP_VSA2	0.51967	0.234576
PEOE_VSA-0	−0.50737	0.229023
PEOE_VSA-3	−0.37201	0.167926
FCharge	−0.2124	0.095876

[a]Descriptor definitions are given in Table S3.

Table 4:

Second-order acylation rates for select cephalosporins against tPBP2[H041]-K361E.

Cephalosporin	R₂	k_2/K_s (M⁻¹s⁻¹)[a]	K361E k_2/K_s (M⁻¹s⁻¹)[b]	Fractional Activity[c]
cefoperazone (CFP)		11,800 ± 1,300	370 ± 60	0.03
ceftriaxone (CRO)		1,710 ± 320	290 ± 70	0.17
ceftazidime (CAZ)		790 ± 150	560 ± 180	0.70
cefepime (FEP)		630 ± 50	410 ± 130	0.64

[a]Second order acylation rate constants against native tPBP2[H041], as reported in Table 1.

[b]The acylation rate constant for each cephalosporin was determined using a gel-based competition assay with Bocillin-FL, as described in Methods. Final values were derived from a minimum of three separate determinations.

[c]The fractional acylation rate compared to that with native tPBP2[H041].